Grid Connected Inverter For A High Reliability Single Phase Transformerless PV Application

[1]Konda Naresh,
[1]Assistant Professor,
[1]Electrical; Engineering of Department,
Hyderabad, India.

Abstract: In This paper, propose a high reliability single phase transformer less grid connected PV Inverter that exploit MOSFETs super junction to attain high frequency, efficiency to application of PV to proposed inverter current fed topology ac-coupled inductor to that operate separately for positive and negative half cycles. to increase the quality of efficiency grid zero crossing instant improving the ac-current quality. even light load operation to achieve high efficiency MOSFET super junction are utilized. The higher operating system cost will reduce. A dual inductor clamped circuit can minimize the system high frequency ac-side switches conducting the current during the current fed topology freewheeling diode this reduce the total cost of the power ground loop leakage the total losses evaluated by conducting several exiting transformer less inverter. efficiencies with an 8-kW converter system from the product datasheet is 98.3% and 98%, respectively, with 345-V dc input voltage and a 16-kHz switching frequency. the simulation part of the experiment has been exclusively in the paper so par utilize MATLAB/PSIM 9.0 the simulation work disposed with this part of the work.

Keywords—Super junction MOSFET, inverter, dual inductor, clamped , freewheeling diode

I. INTRODUCTION

In order to minimize greater ground leakage current and improve the efficiency of the converter system, transformer less PV inverter utilize unipolar PWM control have been presented one commercialized unipolar inverter topology the ground leakage current and use hybrid MOSFET data sheet is 98.3% and 98%, respectively, with 345-V dc input voltage and a 16-kHz however topology has higher conduction losses due to the fact that the current must be conduct through three switches i9n series during the active phase. Line frequency switches S1 and S2 cannot utilize MOSFET device because of the MOSFET BD has slow reverse recovery induce higher turn-on loss. Shoot through issue associate with full bridge Current fed topology PWM inverter remain in the topology due to the fact that three active switches are series connected in the dc bus.

One key issue for high efficiency and reliability transformer less PV inverter achieve a high efficiency over wide range of load necessity to use MOSFET switch.

another key issue of inverter should not have any shoot through issues for higher reliability. in order to proposed single phase PV inverter grid connected system.1) high reliability because there are no shoot through issues,2) low output ac current distortion as a result of no dead time requirements at every PWM switching commutation instant as well as at grid zero crossing instants, 3) minimized CM leakage current because there are two additional ac-side switches that decouple the PV array from the grid during the freewheeling phases converter can reliability employ super junction MOSFETs since it never has the chance to induce MOSFET body diode reverse recovery.

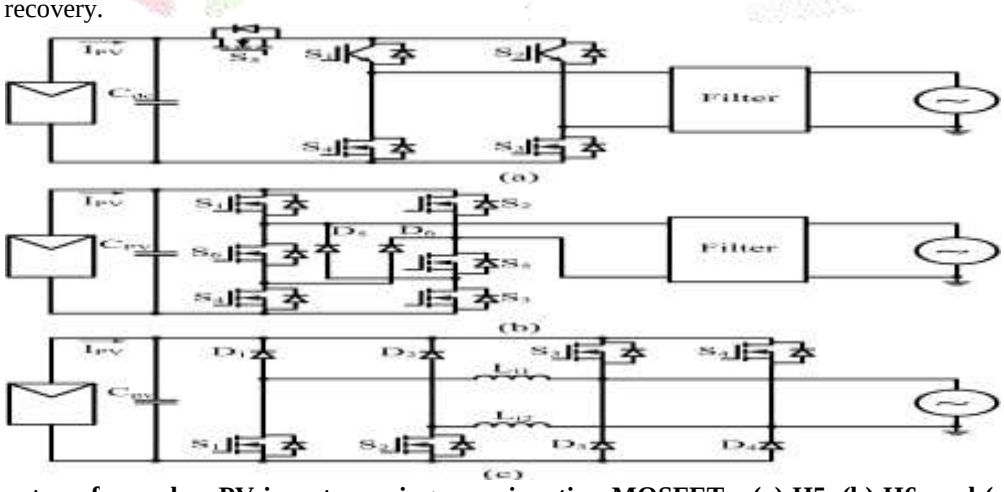

Fig. 1. Single-phase transformerless PV inverters using superjunction MOSFETs: (a) H5, (b) H6, and (c) dual-paralleled-buck inverters.

II. SYSTEM CONTROL

A. Selecting a standalone mode

As shown in the figure the output voltage of the generator is fed to a DC/AC converter that converts a DC output of the generator to be fixed voltage and frequency for utility mains or loads. the DSP controller monitors multiple system variables on a real time basis and excites control routines to optimize the operation of the infidel subsystems in response to measured variables. It also provides all necessary functions to sense output voltages current, and power, to operate protections, and to give reference signals to regulators.

The output power of the converter is controlled according to the reference signal of the control unit. As described above, in order to compensate for reactive power and higher harmonic components for reactive power to improve power factor, the active power (p) and reactive power Ease of Use(Q) should be controlled independently. Moreover, the above system needs over dimensioning some parts.

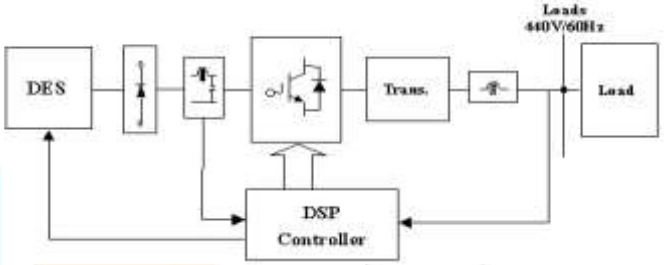

Fig.2.1 Block diagram for standalone mode

B.Maintaining the Integrity of the Specifications

Power Converters supplying power in a standalone mode or feeding it back to the utility mains Fig. shows a block diagram of multiple power converters for a standalone AC system or feeding generated powers back to the utility mains. If all generators are directly connected to the loads, the systems operate as a standalone AC system. Meanwhile, if these are connected in parallel to the mains, these provide the utility grids with an electric power. Each system consists of a generator, an input filter, an AC/AC power converter, an output filter, an isolation transformer, a control unit (DSP), a static switch (SW 1) and output sensors (V, I, P). The function of the static switch (SW 1) is to disrupt the energy flow between the generator and mains or loads in the case of disturbances in the mains voltage. As shown in Fig., this configuration is very similar to parallel operation of multiple UPS systems except that the input sources of inverters are independent generation systems such as micro turbines, fuel cells, and photo voltaic, etc. instead of utility mains.

In case of parallel operation of UPS systems, a recent critical research issue is to share linear and nonlinear load properly by each unit. In general, the load sharing is mainly influenced by non uniformity of the units, component tolerance, and line impedance mismatches. Another issue is a proper control scheme without any control interconnection wires among inverters because these wires restrict the location of the inverter units as well as these can act as a source of the noise and failure. Moreover, in three-phase systems they could also cause unbalance and draw excessive neutral currents.

Even if conventionally passive L-C filters were used to reduce harmonics and capacitors were employed to improve the power factor of the ac loads, passive filters have the demerits of fixed compensation, large size, and resonance. Therefore, the injected harmonic, reactive power burden, unbalance, and excessive neutral currents definitely cause low system efficiency and poor power factor. In particular, a power factor can be improved as AC/AC power converters function a complete active filter for better power quality and the above problems should be overcome by a good control technique to assure the DES to expand increasingly around the world.

$$I_{PV} = I_{Ph} - I_D - I_{sh}$$

$$I_D = I_0\left(e^{\frac{q(V_{PV}+I_{PV}R_S)}{\eta kT}} - 1\right)$$

$$I_{sh} = \frac{V_{PV} + I_{PV}R_S}{R_{sh}}$$

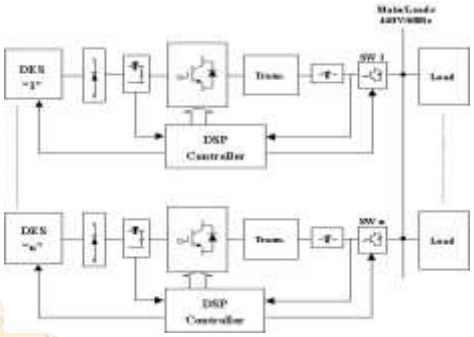

Fig.2.2 Block diagram of power converters connected in parallel

So the above issues can be applied to distributed power systems similarly, and the recent research focuses are summarized as follows:

1. Standardized DES modeling using the software tools
2. Equal load sharing such as the real and reactive power, the load harmonic current among the parallel connected inverters.
3. Connection capability of more DES to the utility mains in best conditions
4. Independent P, Q control of the inverters
5. Power factor correction
6. Reduction of Total Harmonic Distortion (THD).

The aspire of recreational area transform and equations between inverter chipping in and yield, the inverter controller block diagram for supplying reference value .

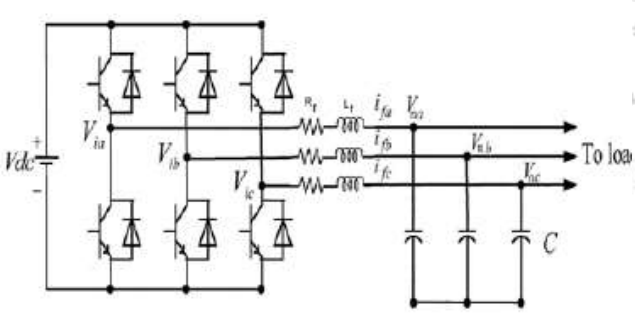

Figure.2.3 PWM inverter diagram

Pref and Qref is as figures. For the current controller, two Proportional-Integral (PI) regulators have been chosen in order to meet the requirements of stability of the system and to make the steady state error be zero. With this control scheme, it is possible to control the inverter in such way that injects reference value of Pref, Qref into other part of stand-alone network.

When the output voltage is needed to be regulated, the PV control scheme that is similar to PQ mode with feedback of voltage used to adjust Qref.

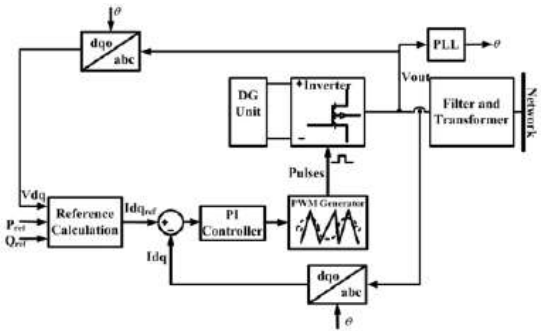

Figure .2.4 : PQ control scheme of inverter

PV Model

The electrical equivalent circuit model of PV cell consists of a current source in parallel with a diode [14] as shown in Fig. 1.

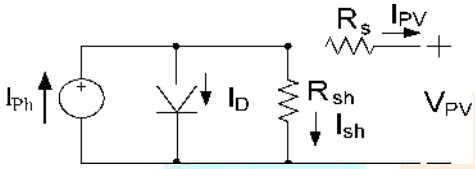

Figure 1 Electrical Equivalent Circuit Model of PV Cell

From the electrical equivalent circuit of the PV cell, PV output current $_{(IPV)}$ is given by

The parameters *q, η, k and T* denote the electronic charge, ideality factor of the diode, Boltzmann constant and temperature in Kelvin respectively. $_{Iph}$ is photocurrent, *I0* is diode reverse saturation current, $_{IPV}$ and $_{VPV}$ are the PV output current and voltage respectively.

As the value of $_{Rsh}$ is very large, it has a negligible effect on the I-V characteristics of PV cell or array. Thus (1) can be simplified to

$$I_{PV} = I_{ph} - I_0\left(e^{\frac{q(V_{PV}+I_{PV}R_S)}{\eta kT}} - 1\right)$$

$$I_{PV} = N_p\left\{Iph - I_0\left(e^{\frac{q(V_{PV}+I_{PV}R_S)}{\eta kTN_S}} - 1\right)\right\}$$

The PV model is simulated using Solarex MSX60, 60W PV module. The simulated I-V and P-V characteristics of the Solarex PV module at constant temperature and varying insolation are shown in Fig. 2(a) and Fig. 2(b) respectively. It can be seen from Fig. 2(a) that the decrease in insulation reduces the current largely but voltage fall is small. Fig. 2(b) shows that the reduction in insolation reduces the power largely as both voltage and current are decreasing.

The effect of temperature on I-V and P-V characteristics of Solarex PV module is shown in Fig. 3(a) and Fig. 3(b) respectively. It can be seen from Fig. 3(a) that the increase in temperature reduces the open circuit voltage largely but rise in current is very small. Fig. 3(b) shows that the increase in temperature reduces the PV output power as the reduction in the voltage is larger than the increase in current due to temperature rise.

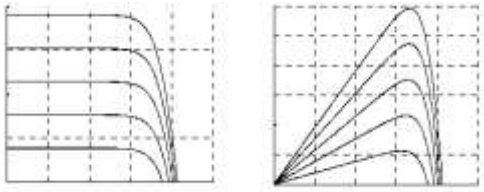

Figure 2 (a) I-V characteristics and (b) P-V characteristics of the Solarex PV

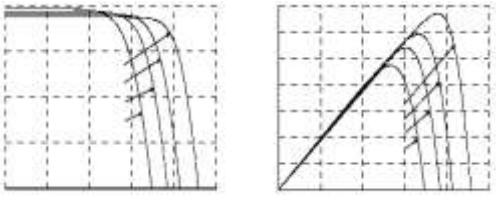

Figure 3 (a) I-V characteristics and (b) P-V characteristics of the Solarex PV module at constant insolation λ =1000W/m2 and different temperature.

When S1 and S3 are ON, diode D5 is reverse-biased, the inductor currents of $_{Lo1}$ and $_{Lo3}$ are equally charged, and energy is transferred from the dc source to the grid; when S1 and S3 are deactivated, the switch S5 and diode D5 provide the inductor current $_{L1}$ and $_{L3}$ a freewheeling path decoupling the PV panel from the grid to avoid the CM leakage current. Coupled-inductor L2 is inactive in the positive half-line grid cycle. Similarly, in the negative half cycle, S2 and S4 are switched at high frequency and S6 remains ON. Freewheeling occurs through S6 and D6.

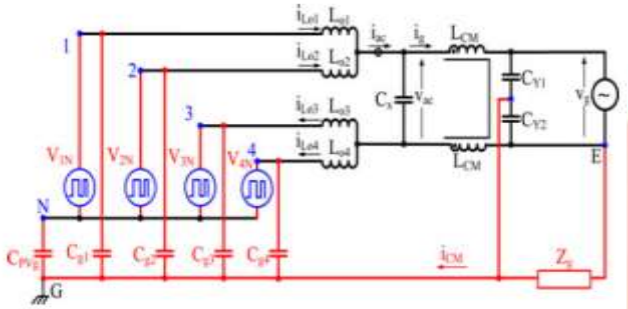

Fig. 7. Leakage current analysis model for the proposed transformerless PV inverter

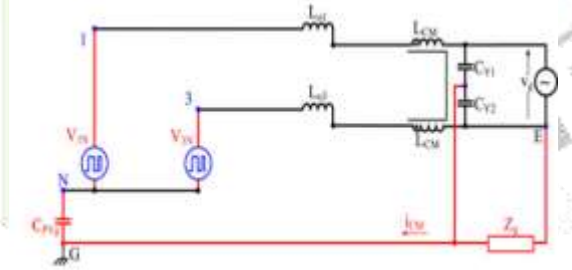

Fig. 6. Simplified CM leakage current analysis model for positive half-line cycle.

CIRCUIT DESIGN

With the help of the CM and DM concepts and by introducing the equivalent circuits between N and E, a single-loop mode applicable to the CM leakage current analysis for the positive half-line cycle of the proposed transformer less inverter is obtained, as shown in Fig. 7, with

$$V_{\mathrm{CM}} = \frac{V_{1N} + V_{3N}}{2} \qquad (1)$$

$$V_{\mathrm{DM}} = V_{1N} - V_{3N}. \qquad (2)$$

$$V_{tCM} = V_{CM} + V_{DM} \cdot \frac{L_{o1} - L_{o3}}{2(L_{o1} + L_{o3})} = \frac{V_{1N} + V_{3N}}{2} + (V_{1N} - V_{3N}) \cdot \frac{L_{o1} - L_{o3}}{2(L_{o1} + L_{o3})}. \quad (3)$$

It is clear that if the total CM voltage v_{tCM} keeps constant, no CM current flows through the converter. For a well-designed circuit with symmetrically structured magnetics, normally $Lo1$ is equal to $Lo3$. During the active stage of the positive half-line cycle, $V1N$ is equal to Vdc, while $V3N$ is equal to 0. Hence, the total CM voltage can be calculated as

$$V_{tCM} = \frac{V_{1N} + V_{3N}}{2} + (V_{1N} - V_{3N}) \cdot \frac{L_{o1} - L_{o3}}{2(L_{o1} + L_{o3})} = \frac{V_{dc}}{2}. \quad (4)$$

During the freewheeling stage of the positive half-line cycle, under the condition that S1 and S3 share the dc-link voltage equally when they are simultaneously turned OFF, one can obtain

$$V_{1N} = V_{3N} = \frac{V_{dc}}{2}. \quad (5)$$

Therefore, the total CM voltage during the freewheeling stage is calculated as

$$V_{tCM} = \frac{V_{1N} + V_{3N}}{2} + (V_{1N} - V_{3N}) \cdot \frac{L_{o1} - L_{o3}}{2(L_{o1} + L_{o3})} = \frac{V_{dc}}{2}. \quad (6)$$

Equations (4) and (6) indicate that the total CM voltage keeps constant in the whole positive half-line cycle. As a result, no CM current is excited. Similarly, during the whole negative half-line cycle, the CM leakage current mode is exactly the same as the one during the positive half-line cycle; the only difference is the activation of different devices. The total CM voltage in the negative half-line cycle is also equal to $V_{dc}/2$. Therefore

TABLE I
SPECIFICATIONS AND POWER DEVICES FOR EFFICIENCY EVALUATION

Nominal input voltage	380V
Grid voltage	240Vac
Nominal frequency	60Hz
Nominal output power	5 kW
Nominal AC current	21A
Switching frequency	20kHz
MOSFETs	IPW60R041C6
IGBTs	IRGB4063D
Diodes	APT30DQ60B

B. Calculation and Comparison of the Power Semiconductor Device Losses for Several Existing MOSFET Transformerless Inverters

Since the efficiency of PV transformerless inverters is normally compared by using weighted efficiency concepts, such as "CEC Efficiency" and "EU Efficiency," it is critical to evaluate power semiconductor device losses at different load conditions rather than at nominal load condition when evaluating the efficiency of MOSFET transformerless PV inverters. The specifications and power devices

for efficiency evaluation of several existing MOSFET transformerless PV inverters [11]–[13] and the proposed inverter are listed in Table I.

The first-order conduction voltage drop models of semiconductor devices can be given by

$$\text{MOSFET}: v_{ds}(t) = i(t) \cdot R_{ds} \quad (7)$$

$$\text{IGBT}: v_{ce}(t) = V_t + i(t) \cdot R_{ce} \quad (8)$$

$$\text{Diode}: v_{ak}(t) = V_f + i(t) \cdot R_{ak} \quad (9)$$

where v_{ds} is the MOSFET drain–source voltage drop, R_{ds} is the MOSFET drain–source on resistance, v_{ce} is the IGBT collector–emitter voltage drop, V_t is the IGBT equivalent voltage drop under zero current condition, R_{ce} is the IGBT on resistance, v_{ak} is the diode anode–cathode voltage drop, V_f is the diode equivalent voltage drop under zero current condition, and R_{ak} is diode on resistance; $i(t)$ is the inverter output current and expressed as

$$i(t) = I_m \cdot \sin(\omega t) \quad (10)$$

where I_m is the peak inverter output current and ω is the angular frequency of the inverter output current.

The duty ratios for active-stage devices and zero-stage devices of unipolar grid-connected PWM inverters are expressed as (11) and (12), respectively

$$d_{active}(t) = M \sin(\omega t) \quad (11)$$

$$d_{zero}(t) = 1\ M \sin(\omega t). \quad (12)$$

The conduction losses for active-stage MOSFET switches, active-stage IGBT switches, zero-stage MOSFET switches, zero-stage IGBT switches, and zero-stage diodes can be calculated, respectively, from (13) to (17)

$$P_{con\_active\_MOSFET} = \frac{1}{2\pi}\int_0^{\pi} i(t)v_{ds}(t)d_{active}(t)d\omega t = I_m^2 R_{ds}\frac{2M}{3\pi} \quad (13)$$

$$P_{con\_active\_IGBT} = \frac{1}{2\pi}\int_0^{\pi} i(t)v_{ce}(t)d_{active}(t)d\omega t = I_m V_t \frac{M}{4} + I_m^2 R_{ce}\frac{2M}{3\pi} \quad (14)$$

$$P_{con\_zero\_MOSFET} = \frac{1}{2\pi}\int_0^{\pi} i(t)v_{ds}(t)d_{zero}(t)d\omega t = I_m^2 R_{ds}\left(\frac{1}{4} - \frac{2M}{3\pi}\right) \quad (15)$$

$$P_{con\_zero\_IGBT} = \frac{1}{2\pi}\int_0^{\pi} i(t)v_{IGBT}(t)d_{zero}(t)d\omega t = I_m V_t\left(\frac{1}{\pi} - \frac{M}{4}\right) + I_m^2 R_{ce}\left(\frac{1}{4} - \frac{2M}{3\pi}\right) \quad (16)$$

$$P_{con\_zero\_Diode} = \frac{1}{2\pi}\int_0^{\pi} i(t)v_{ak}(t)(1 - M\sin(\omega t))d\omega t = I_m V_f\left(\frac{1}{\pi} - \frac{M}{4}\right) + I_m^2 R_{ak}\left(\frac{1}{4} - \frac{2M}{3\pi}\right). \quad (17)$$

V.CONCLUSION

This paper has In This paper, propose a high reliability single phase transformer less grid connected PV Inverter that exploit MOSFETs super junction to attain high frequency, efficiency to application of PV to proposed inverter current fed topology ac-

coupled inductor to that operate separately for positive and negative half cycles. to increase the quality of efficiency grid zero crossing instant improving the ac-current quality. even light load operation to achieve high efficiency MOSFET super junction are utilized. The higher operating system cost will reduce. A dual inductor clamped circuit can minimize the system high frequency ac-side switches conducting the current during the current fed topology freewheeling diode this reduce the total cost of the power ground loop leakage the total losses evaluated by conducting several exiting transformer less inverter. efficiencies with an 8-kW converter system from the product datasheet is 98.3% and 98%, respectively, with 345-V dc input voltage and a 16-kHz switching frequency. the simulation part of the experiment has been exclusively in the paper so par utilize MATLAB/PSIM 9.0 the simulation work disposed with this part of the work. The control goals had been dissected and it is inferred that the control loop must give exact phase and amplitude regulation. In this way a present control loop with PI controller is proposed.

The extension of this work might focus on the following aspects:

- Feedback control of the dc-link voltage ripple.

REFERENCES

[1] S. Lee, G. Son, and J.-W. Park, "Power management and control for grid-connected DGs with intentional islanding operation of inverter," IEEE Trans. Power Systems, vol. 28, no. 2, pp. 1235–1244, May 2013.

[2] P. Xuewei and A. K. Rathore, "Small Signal Modeling of Snubberless Soft-switching Current-fed Bidirectional Converter and Control Implementation using PSoC," IEEE Transactions on Vehicular Technology, vol. 64, no. 11,Nov 2015, pp. 4996-5005.

[3] Ravi Bukya and Prof B.Mangu, "Soft-Switching Snubberless Current fed half bridge DC-DC Converter For PV Application" IEEE Conference on ICITE-2018 ,Apr-18.

[4] Shih-Jen Cheng; Yu-Kang Lo; Huang-Jen Chiu; Shu-Wei Kuo, "High- Efficiency Digital-Controlled Interleaved Power Converter for High- Power PEM Fuel-Cell Applications," IEEE Transactions on Industrial Electronics, vol.60, no.2, pp.773-780, Feb. 2013.

[5] P. Xuewei and A. K. Rathore, "Naturally Clamped Zero Current Commutated Soft-switching Current-fed Push-Pull DC/DC Converter: Analysis, Design, and Experimental Results," IEEE Transactions on Power Electronic, Vol. 30, no. 3, March 2015, pp. 1318-1327.

[6] S. Bal, A. K. Rathore, and D. Srinivasan, "Naturally commutated current-fed three-phase bidirectional soft-switching dc-dc converter with 120^o modulation technique," *in Press, IEEE Transactions on Industry Applications, Jan 2016.*

[7] S. Bal, A. K. Rathore, D. Srinivasan, "Naturally clamped snubberless soft-switching bidirectional current-fed three-phase push-pull dc/dc converter for dc microgrid application," *IEEE Transactions on Industry Applications*, vol. 52, no. 2, March/April 2016, pp. 1577-1587.